Scientific Report

SOURCE DATA | TRANSPARENT PROCESS

EMBO reports

The antiobesity factor WDTC1 suppresses adipogenesis via the CRL4^{WDTC1} E3 ligase

Beezly S Groh[1], Feng Yan[2], Matthew D Smith[2], Yanbao Yu[1], Xian Chen[1] & Yue Xiong[1,2,*]

Abstract

***WDTC1/Adp* encodes an evolutionarily conserved suppressor of lipid accumulation. While reduced *WDTC1* expression is associated with obesity in mice and humans, its cellular function is unknown. Here, we demonstrate that WDTC1 is a component of a DDB1-CUL4-ROC1 (CRL4) E3 ligase. Using 3T3-L1 cell culture model of adipogenesis, we show that disrupting the interaction between WDTC1 and DDB1 leads to a loss of adipogenic suppression by WDTC1, increased triglyceride accumulation and adipogenic gene expression. We show that the CRL4^{WDTC1} complex promotes histone H2AK119 monoubiquitylation, thus suggesting a role for this complex in transcriptional repression during adipogenesis. Our results identify a biochemical role for WDTC1 and extend the functional range of the CRL4 complex to the suppression of fat accumulation.**

Keywords adipose; adp; cullins; obesity; WDTC1

Subject Categories Metabolism; Post-translational Modifications, Proteolysis & Proteomics

DOI 10.15252/embr.201540500 | Received 6 April 2015 | Revised 25 February 2016 | Accepted 4 March 2016 | Published online 9 April 2016

EMBO Reports (2016) 17: 638–647

Introduction

Over 50 years ago, Dr. Winifred Doane isolated and extensively characterized a naturally derived *D. melanogaster* mutant, termed *adipose* (*adp*) [1,2]. The most obvious mutant phenotype observed was fat body hypertrophy due to excessive lipid storage. *Adp* is evolutionarily conserved from files to humans as a single gene and encodes a protein containing WD40 repeat domains and TPR motifs [3]. The mammalian homolog of *Adp* is *WDTC1* (WD40 and tetratricopeptide repeats 1). Loss of a single *Wdtc1* allele results in obese mice with poor metabolic profiles, and conversely, transgenic expression of *Wdtc1* in fat cells yields lean mice [4]. Recently, population studies have linked reduced *WDTC1* expression to human obesity [5,6]. Despite strong genetic evidence linking WDTC1 to antiadipogenic function, its molecular mechanism remains unknown.

Ubiquitin pathway plays a critical role in virtually all cellular processes. Ubiquitylation proceeds via an enzymatic cascade where E1 and E2 enzymes catalyze the activation and conjugation of ubiquitin, while E3s confer reaction specificity through substrate recruitment [7,8]. Substrates can be polyubiquitylated, which often leads to proteasome-dependent degradation, or monoubiquitylated, which regulates the property and thus the function of the substrate. Comprising the largest family of E3 ligases is the cullin RING E3 ligase (CRL) complexes in which a cullin serves as the scaffold to bind small RING finger protein ROC1 (RBX1/HRT1) through a C-terminal domain, and a linker-substrate receptor dimer or a substrate receptor directly via a N-terminal domain. Mammalian cells express two cullin 4 (CUL4) proteins, CUL4A and CUL4B, that bind damaged DNA binding (DDB1) protein. DDB1 acts as the linker to bridge the interaction between CUL4 and a subset of DDB1 binding WD40 repeat proteins (DWDs or DCAFs for DDB1 cullin-associated factors) which function as substrate receptors to target specific substrates to the CRL4 E3 complexes [9–12]. The human genome encodes an estimated ~90 DWD proteins [9], but the functional interaction between CRL4 and DWDs remains unexplored for the vast majority. One of predicted DWD protein is WDTC1, raising the possibility that WDTC1 may function as a substrate receptor of CRL4 E3 ligase to inhibit fat accumulation. This study is aimed at determining this issue.

Results and Discussion

WDTC1 is a putative substrate receptor for CRL4 E3 ligase

Two structural features suggested that WDTC1 binds DDB1 (Fig 1A). First, WDTC1 contains two tandem DWD boxes with conserved WDXR submotifs, the signature motif present in nearly all WD40 proteins that bind DDB1 [9]. Second, the N-terminal regions of vertebrate WDTC1 contain an α-helical motif termed the H-box which is shared by several DWD proteins and some viral proteins that bind DDB1 [13]. Although the H-box of the DWD protein DDB2 makes a large contribution to DDB1 binding [11,13], a mutation in the WDXR of DDB2 (R273) is found in human xeroderma pigmentosum patients and disrupts DDB2-DDB1 binding [14]. These observations underscore the importance and specificity of both DWD motif and H-box in mediating DDB1 binding, thus offering a unique opportunity for investigating the WDTC1–CRL4 interaction.

1 Department of Biochemistry and Biophysics, University of North Carolina, Chapel Hill, NC, USA
2 Lineberger Comprehensive Cancer Center, University of North Carolina, Chapel Hill, NC, USA
*Corresponding author. Tel: +1 919 962 2142; Fax: +1 919 966 8799; E-mail: yxiong@email.unc.edu

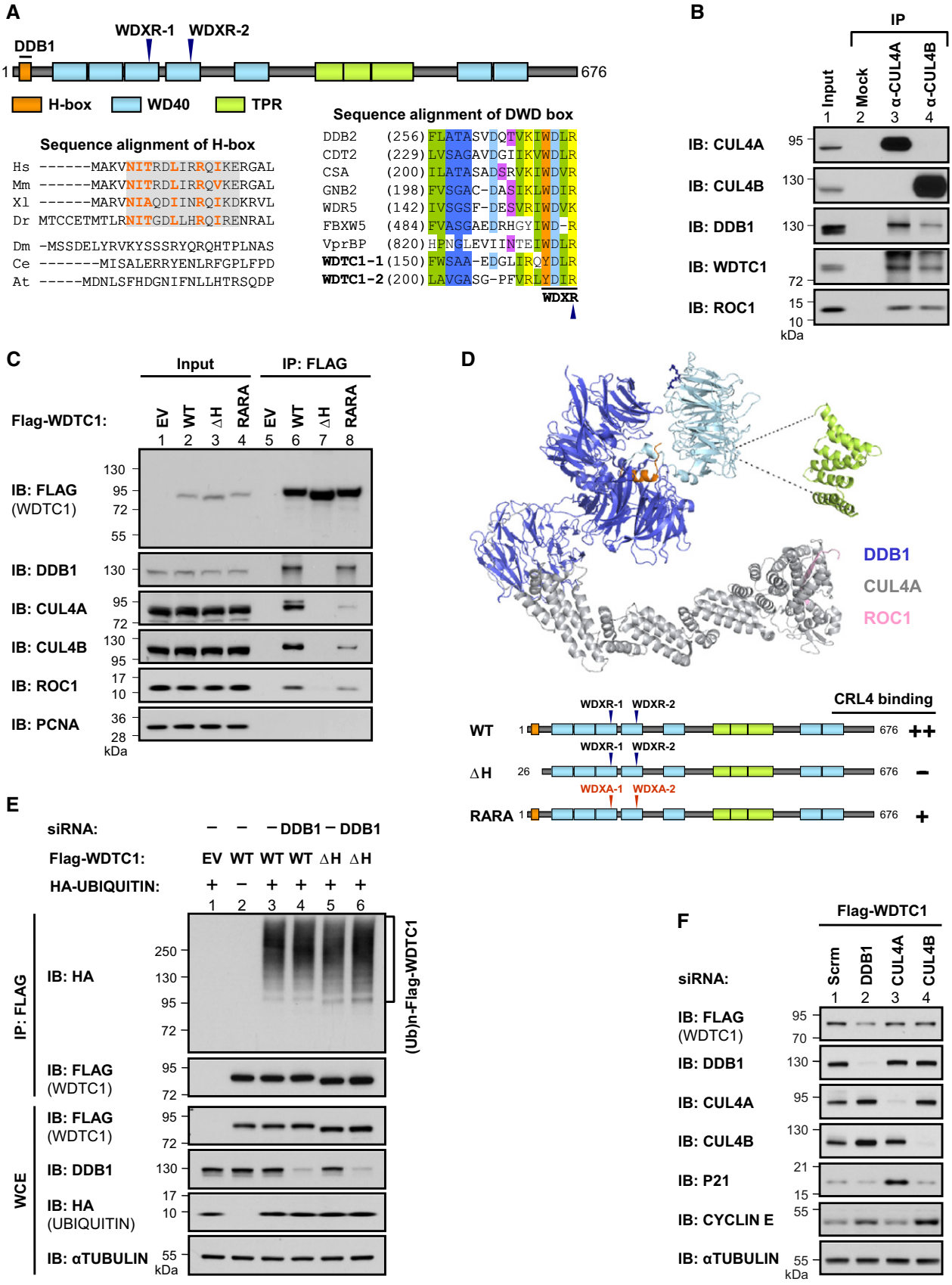
A
DDB1
WDXR-1
WDXR-2
1
676
H-box
WD40
TPR
Sequence alignment of H-box
Hs ------MAKVNITRDLIRRQIKERGAL
Mm ------MAKVNITRDLIRRQVKERGAL
Xl ------MARVNIAQDIINRQIKDKRVL
Dr MTCCETMTLRNITGDLLHRQIRENRAL
Dm -MSSDELYRVKYSSSRYQRQHTPLNAS
Ce -------MISALERRYENLRFGPLFPD
At -----MDNLSFHDGNIFNLLHTRSQDP
Sequence alignment of DWD box
DDB2 (256) FLATASVDQTVKIWDLR
CDT2 (229) LVSAGAVDGIIKVWDLR
CSA (200) ILATASADSRVKIWDVR
GNB2 (198) FVSGAC-DASIKLWDIR
WDR5 (142) IVSGSF-DESVRIWDVK
FBXW5 (484) FVASGAEDRHGYIWD-R
VprBP (820) HPNGLEVIINTEIWDLR
WDTC1-1 (150) FWSAA-EDGLIRQYDLR
WDTC1-2 (200) LAVGASG-PFVRLYDIR
WDXR
B
IP
Input
Mock
α-CUL4A
α-CUL4B
1 2 3 4
IB: CUL4A
IB: CUL4B
IB: DDB1
IB: WDTC1
IB: ROC1
95
130
130
72
15
10
kDa
C
Input
IP: FLAG
Flag-WDTC1:
EV WT ΔH RARA EV WT ΔH RARA
1 2 3 4 5 6 7 8
IB: FLAG (WDTC1)
IB: DDB1
IB: CUL4A
IB: CUL4B
IB: ROC1
IB: PCNA
130 95 72 55
130
95 72
130 95
17 10
36 28
kDa
D
DDB1
CUL4A
ROC1
CRL4 binding
WT 1 WDXR-1 WDXR-2 676 ++
ΔH 26 WDXR-1 WDXR-2 676 −
RARA 1 WDXA-1 WDXA-2 676 +
E
siRNA: − − − DDB1 − DDB1
Flag-WDTC1: EV WT WT WT ΔH ΔH
HA-UBIQUITIN: + − + + + +
1 2 3 4 5 6
IP: FLAG
IB: HA
IB: FLAG (WDTC1)
WCE
IB: FLAG (WDTC1)
IB: DDB1
IB: HA (UBIQUITIN)
IB: αTUBULIN
250 130 95 72
95 72
95 72
130
17 10
55
kDa
(Ub)n-Flag-WDTC1
F
Flag-WDTC1
siRNA:
Scrm DDB1 CUL4A CUL4B
1 2 3 4
IB: FLAG (WDTC1)
IB: DDB1
IB: CUL4A
IB: CUL4B
IB: P21
IB: CYCLIN E
IB: αTUBULIN
95 70
130
95
130
21 15
55
55
kDa

Figure 1.

Figure 1. WDTC1 is a substrate receptor of CRL4 E3 complexes.

A Domain structure of human WDTC1 with locations of the H-box and WDXR motifs indicated. Alignment of WDTC1 H-box motifs in different species (boxed in gray) and bolded orange represents key residues contacting DDB1 [13]. Alignment of DWD boxes in different DWD proteins (bottom right) with WDXR submotif indicated; tandem DWD boxes are shown for WDTC1 only.

B Endogenous CUL4A and CUL4B complexes were isolated from 293T cell lysates by immunoprecipitation (IP), and associated proteins were detected by immunoblotting (IB). Mock includes beads only control.

C Flag-tagged WT and mutant WDTC1 proteins were transiently expressed in 293T cells. Flag-WDTC1 complexes were immunoprecipitated with anti-FLAG, and their associated proteins were detected by immunoblotting as indicated; EV, empty vector control.

D Top, the modeled structure of WDTC1 in complex with CRL4 (PDB 4A0K); WDTC1 superimposition was based on its H-box (PDB 317N). WDTC1 domains are rendered in same colors as linear domain structure in (A); WDXR arginines were rendered in dark blue ball-and-stick. Bottom, schematic summarizing results presented in (C).

E 293T cells were transfected with HA-ubiquitin along with various combinations of plasmid and siRNA as indicated. Transfected cells were lysed under denaturing conditions to obtain whole-cell extracts (WCE) and immunoprecipitated with anti-FLAG. WDTC1 ubiquitylation was evaluated by immunoblotting as indicated.

F 293T cells transiently expressing Flag-WDTC1 were transfected with scramble (scrm) siRNA or siRNAs against DDB1, CUL4A, and CUL4B. Flag-WDTC1 levels and knockdown efficiency were assessed by immunoblotting as indicated.

Source data are available online for this figure.

To test whether WDTC1 and CRL4 interact *in vivo*, endogenous CUL4A or CUL4B complexes were immunoprecipitated from 293T cells, and the presence of WDTC1 in the immunoprecipitates was determined by immunoblotting. We found that WDTC1 interacts endogenously with both CUL4A and CUL4B (Fig 1B). We then generated two WDTC1 mutants, one deleted the N-terminal 25 amino acid residues containing the H-box (referred to as ΔH) and one substituted the arginine residues in the tandem WDXR motifs to alanines (referred to as RARA; Fig 1A). We found that wild-type Flag-WDTC1 coimmunoprecipitated all CRL4 subunits tested, including DDB1, CUL4A, CUL4B, and ROC1 (Fig 1C). In contrast, deletion of the H-box (ΔH) completely ablated complex formation, while the RARA mutant showed a modest decrease in DDB1 binding and a marked reduction in CUL4 and ROC1 binding. A superimposed structure of WDTC1 is shown in complex with CRL4 (Figs 1D and EV1). As previously reported [13], WDTC1 is anchored through its H-box into the BPC propeller domain of DDB1. Similar to DDB2-DDB1 binding [15], the tandem WDXRs of WDTC1 are not predicted to make direct contact with DDB1 but are solvent-exposed on the bottom surface of the β-propeller. How these two signature arginine residues contribute to the binding of DWDs to DDB1 is presently unclear.

We previously reported an example of a DWD protein, WDR5, that is ubiquitylated by its cognate CRL4B and targeted for proteolysis [16]. We therefore tested whether WDTC1 is a CRL4 substrate by *in vivo* ubiquitylation assays. We found that WDTC1 was extensively ubiquitylated, but the levels were unchanged by either DDB1 knockdown or ΔH mutation (Fig 1E). Further, the steady-state levels of Flag-WDTC1 protein were largely unaltered by CUL4A or CUL4B knockdown, while their respective substrates p21 and cyclin E were clearly stabilized (Fig 1F), indicating that CRL4 does not regulate WDTC1 protein stability. We noted that DDB1 depletion resulted in a slight decrease in Flag-WDTC1, possibly due to protein instability arising from the near loss of its primary binding partner. Together, these results demonstrate that WDTC1 is a component of DDB1-CUL4A/B-ROC1 complexes and likely functions as a substrate receptor of CRL4 E3 ligases.

The interaction of WDTC1 with CRL4 is critical for its function in adipogenic suppression

To determine the biological significance of the CRL4–WDTC1 interaction, we hypothesized that the fat-suppressive role of WDTC1 is mediated through CRL4. We first examined the expression of WDTC1 and other CRL4 subunits in mouse tissues, including multiple adipose tissues. We found that DDB1, ROC1 and at least one CUL4 are expressed in all four fat tissues, along with readily detected expression of WDTC1 (Fig EV2A). We then assayed the adipogenic differentiation of 3T3-L1 preadipocytes, the well-characterized cell culture model to study adipogenesis (Fig EV2B). Thought to closely recapitulate adipogenesis *in vivo*, treating 3T3-L1 cells to an adipogenic media triggers transcriptional activation of the terminal differentiation program and morphological changes following lipogenic accumulation of triglycerides [17].

We first confirmed that WDTC1 forms endogenous CRL4 complexes in 3T3-L1 cells (Figs 2A and EV2C). We next evaluated the effects of disrupting the WDTC1–DDB1 interaction on WDTC1 function during adipogenesis. For this purpose, we generated stable 3T3-L1 cells that express a vector control and flag-tagged wild-type (WT), ΔH, or RARA mutant WDTC1 (Fig EV2D) and verified that their expression did not significantly alter the cell cycle distribution (Fig EV2E). When these cells were adipogenically induced, WT WDTC1 suppressed adipogenesis as assessed by Oil Red O staining (ORO; Fig 2B). In striking contrast, $WDTC1^{\Delta H}$ expression promoted adipogenesis, suggesting that it may function as a dominant negative form of WDTC1. Further, the expression of $WDTC1^{RARA}$ mutant also promoted adipogenesis, but at a lower efficiency than $WDTC1^{\Delta H}$. While the $WDTC1^{\Delta H}$ mutant exhibits near-complete loss of DDB1 binding, the $WDTC1^{RARA}$ mutant is partially defective in DDB1 binding, suggesting that $WDTC1^{RARA}$ mutant is functionally equivalent to a hypomorphic allele. This is consistent with genetic evidence indicating that WDTC1 exhibits dosage sensitivity [1,4]. Additionally, WDTC1 likely acts downstream of the insulin signaling pathway as replacing insulin with the PPARγ agonist rosiglitazone did not alter the observed ORO phenotypes (Fig EV2F). Validating the phenotypes evaluated by ORO, ectopic expression of WT WDTC1 suppressed triglyceride accumulation, while expression of the $WDTC1^{\Delta H}$ (3.5-fold) and $WDTC1^{RARA}$ (2.3-fold) mutants resulted in significantly higher triglyceride levels (Fig 2C). Further, expression of WT WDTC1 decreased adipogenic marker expression but $WDTC1^{\Delta H}$ and $WDTC1^{RARA}$ mutants increased the expression of these genes with $WDTC1^{\Delta H}$ again being more effective than $WDTC1^{RARA}$ (Figs 2D and EV2G). We also assessed expression of genes regulating lipogenesis, lipolysis, and fatty acid oxidation, and

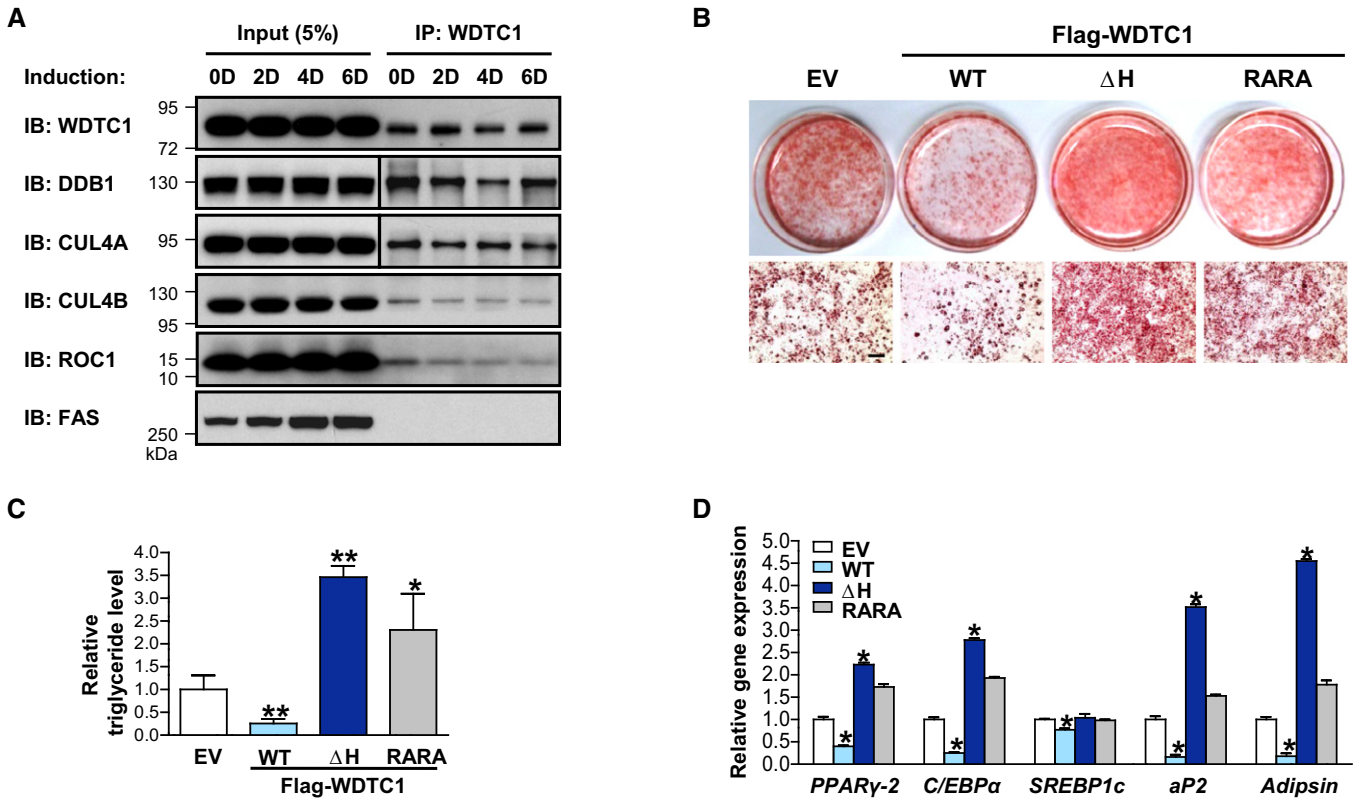

Figure 2. WDTC1 suppresses adipogenesis in a CRL4-dependent manner.

A 3T3-L1 preadipocytes were adipogenically induced, and lysates were prepared from cells collected at indicated days. Endogenous WDTC1 interaction with CRL4 subunits was evaluated by immunoprecipitation with anti-WDTC1 followed by immunoblot analyses with the indicated antibodies. Fatty acid synthase (FAS) levels were monitored to evaluate induction.

B–D 3T3-L1 stable cells expressing vector control (EV), Flag-tagged WT or mutant WDTC1 proteins were adipogenically induced. Adipogenesis was assessed by Oil Red O staining (ORO) (B); plate (top) and microscopic (bottom) views, 0.1 mm scale bar. Triglyceride levels were quantified by an enzymatic assay (C). Adipogenic gene expression was evaluated by RT–qPCR analysis (D).

Data information: In (C, D), bars represent the mean ± SEM from 3 independent experiments. *$P < 0.05$, **$P < 0.005$, significant change compared to EV control. Statistical significance was analyzed by paired two-tailed Student's *t*-tests.
Source data are available online for this figure.

found modest alterations that are likely due to altered adipogenesis in cells expressing WT or mutant WDTC1 proteins (Fig EV2H). The expression of WT WDTC1 resulted in a modest reduction in the expression of genes linked to lipogenesis (*Fasn*, *Dgat1,* and *Dgat2*), lipolysis (*Agtl*) and β-oxidation of long-chain fatty acids (*Cpt2*), while the expression of WDTC1$^{\Delta H}$ led to opposite changes in the expression of these genes. Together, these results support the idea that the CRL4 interaction is critically important for WDTC1 function in the negative regulation of adipogenesis.

CRL4 binding mutants of WDTC1 cannot rescue WDTC1 function

To further validate the functional link between WDTC1 and CRL4 in the suppression of 3T3-L1 adipogenesis, we sought to study the effect of CUL4 knockdown on 3T3-L1 adipogenesis (Fig EV3A). The depletion of CUL4A resulted in a hyperproliferation phenotype, while CUL4B depletion resulted in a cell cycle defect and reduced cell proliferation (Fig EV3B and C). Oil Red O staining indicates that while 3T3-L1 adipogenesis was enhanced by CUL4A depletion, it was substantially inhibited by CUL4B depletion (Fig EV3D). It is presently unclear to us why the knockdown of *Cul4a* and *Cul4b* has opposite effects on 3T3-L1 adipogenesis. However, the function of CUL4A in promoting adipogenesis needs to be cautiously interpreted as it is likely that multiple distinct CRL4A complexes are assembled in 3T3-L1 cells.

To more specifically demonstrate the function of CUL4–WDTC1 interaction in the suppression of 3T3-L1 adipogenesis, we therefore carried out rescue experiments. Utilizing a lentiviral knockdown-rescue vector strategy [18], we engineered 3T3-L1 cells to simultaneously knockdown endogenous *Wdtc1* by shRNA and ectopically re-express shRNA-resistant *WDTC1* encoding either WT or DDB1-binding mutants ΔH or RARA to levels comparable to endogenous WDTC1 (Fig 3A). We found that knocking down *Wdtc1* dramatically enhanced 3T3-L1 differentiation as assayed by ORO (Fig 3B), triglyceride accumulation (Fig 3C), and adipogenic gene expression (Fig 3D). While the re-expression of WT WDTC1 almost completely rescued the loss of adipogenic suppression in all three assays, adding back either ΔH or RARA mutants failed to

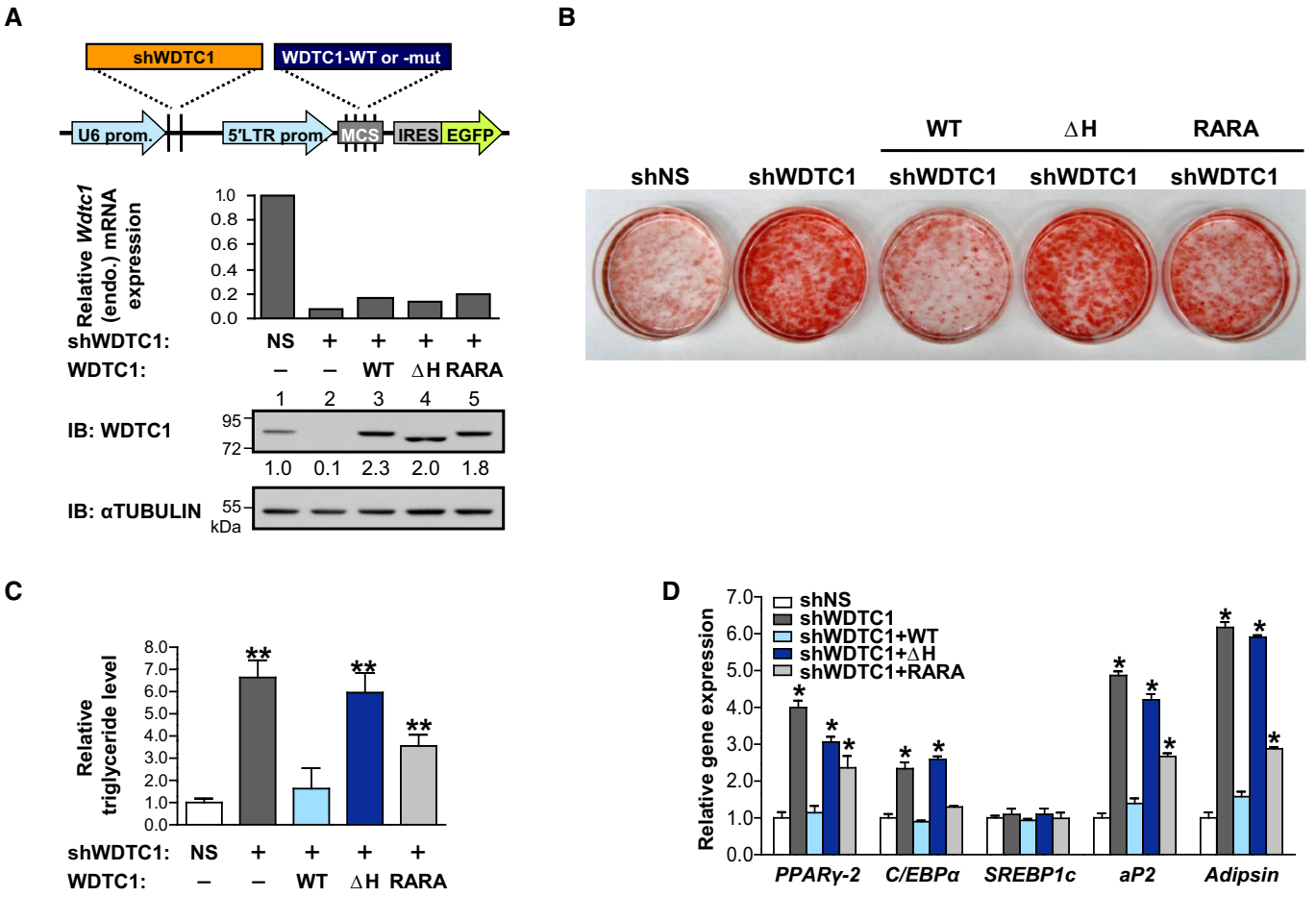

Figure 3. CRL4 binding mutants of WDTC1 cannot rescue WDTC1 knockdown phenotype.

A Schematic of WDTC1 knockdown-rescue lentiviral vector (top). 3T3-L1 preadipocytes were lentivirally transduced to generate stable cells expressing a non-specific (NS) shRNA control, shWDTC1 targeting endogenous *Wdtc1* mRNA, or cells simultaneously expressing shWDTC1 and shRNA-resistant *WDTC1*; bottom, confirmation of knockdown and WDTC1 ectopic expression.

B–D 3T3-L1 stable cells described in (A) were adipogenically induced. Their adipogenic potential was assessed by ORO (B), triglyceride quantitation (C), and adipogenic gene expression (D).

Data information: In (C, D), bars represent the mean ± SEM from 3 independent experiments. *$P < 0.05$, **$P < 0.005$, significant change compared to NS control. Statistical significance was analyzed by paired two-tailed Student's *t*-tests.
Source data are available online for this figure.

rescue the adipogenic defects resulting from the depletion of endogenous *Wdtc1*. Consistent with its partial disruption of DDB1 binding, the RARA mutant exhibited a weaker phenotype than the ΔH mutant, supporting the interpretation that the RARA mutant represents a hypomorphic form of WDTC1, while the ΔH mutant acts as a dominant negative. Collectively, these results demonstrate a strong parallel between $CRL4^{WDTC1}$ complex formation and WDTC1 function, underscoring the critical importance of the CRL4–WDTC1 interaction to the observed adipogenic suppression by WDTC1.

$CRL4^{WDTC1}$ promotes histone H2AK119 ubiquitylation

To gain insight into the mechanism by which $CRL4^{WDTC1}$ suppresses adipogenesis, we carried out two independent coupled immunoprecipitation and mass spectrometry (IP-mass spec) analyses of WDTC1 complexes in 3T3-L1 cells. Validating the IP-mass spec analyses, several known $CRL4^{WDTC1}$ components were identified, including DDB1, CUL4B, CUL4A, ROC1, and all nine subunits of COP9 signalosome subunits (Fig EV4A). One potential novel WDTC1-interacting protein is fatty acid synthase (FAS), a critical and positive regulator of lipid accumulation. We hypothesized that regulation of FAS by the $CRL4^{WDTC1}$ complex may contribute to the antiadipogenic action of WDTC1. We therefore characterized the interaction between WDTC1 and FAS and performed preliminary characterization of a few other candidates as well. However, our data showed that $CRL4^{WDTC1}$ E3 ligase does not appear to regulate FAS steady-state protein levels and reached similar conclusions for other candidates we examined such as HDAC3 and PPARγ-2 (Fig EV4B–D).

We then investigated the possibility that histone H2A is a $CRL4^{WDTC1}$ substrate. This was inspired in part by the established

role of H2AK119 monoubiquitylation (referred to as H2AK119ub1 hereafter) as a key transcription repressive mechanism in the control of development and differentiation, and also because it has been demonstrated that the antiadipogenic function of WDTC1 is lost upon nuclear exclusion and WDTC1 physically interacts with ectopically expressed histones [4]. Further, ectopic WDTC1 expression is associated with reduced adipogenic marker expression (Fig 2D; [4]).

We first examined the subcellular distribution of Flag-WDTC1 and found that while it is abundantly recovered in the cytosolic fraction, it is also clearly present in the nuclear fractions, and in the MNase-digested chromatin fraction (Fig 4A). We then performed immunoprecipitation experiments with nuclear extracts and demonstrated that WDTC1 associated with H2A, as well as H2B and H3 (Fig 4B). In this experiment, we noted that WDTC1 interacted with H2A, but not the presumably monoubiquitylated form of H2A, an observation that is consistent with the possibility that $CRL4^{WDTC1}$ catalyzes H2AK119ub1. Chromatin coimmunoprecipitation assay confirmed the binding between WDTC1 and nucleosomal histones *in vivo* at physiologic levels (Fig EV4E). Notably, the DDB1 binding mutant, $WDTC1^{\Delta H}$, retained histone binding activity, indicating that histone binding is independent of CRL4 binding. Because $WDTC1^{\Delta H}$ mutant disrupts DDB1 binding and thus disrupts probable ubiquitylation activity, and appears to functionally antagonize WDTC1 during adipogenesis, we took advantage of this mutant to investigate the effect of WDTC1 expression on histone H2AK119ub1 levels. We examined the global level of H2AK119ub1 in preadipocyte and induced 3T3-L1 cells stably expressing either a vector control, WT WDTC1 or $WDTC1^{\Delta H}$ mutant (Fig 4C). We did not detect a notable change in H2AK119ub1 levels among these cell lines in the preadipocyte state. In contrast, expression of WT WDTC1 resulted in a modest, but significant and reproducible, increase in H2AK119ub1 while $WDTC1^{\Delta H}$ expression caused a slight decrease of H2AK119ub1. This result suggests that WDTC1-promoted H2AK119ub1 is linked to adipogenesis and is dependent on the association with the CRL4 E3 complex.

To test whether H2AK119 is a direct target of $CRL4^{WDTC1}$ E3 ligase, we performed *in vitro* ubiquitylation assays. We affinity-purified Flag-tagged WT WDTC1 or $WDTC1^{\Delta H}$ complexes from 293T cells and confirmed the presence of CRL4 components in the WT, but not ΔH, WDTC1 eluted fraction (Fig 4D, left). Recombinant H2A was incubated with purified WDTC1 complexes and reaction products were resolved by SDS–PAGE, followed by immunoblotting with H2AK119ub1 antibodies. The results show that H2A is robustly ubiquitylated by WT WDTC1, but not $WDTC1^{\Delta H}$ complexes (Figs 4D, right, and EV4F), demonstrating that H2A was a specific substrate of $CRL4^{WDTC1}$ in this *in vitro* system. We noted that multiple ubiquitylated H2A forms were detected, perhaps due to the high efficiency nature of *in vitro* ubiquitylation reactions. To confirm that K119 residue is the primary target of $CRL4^{WDTC1}$, wild-type H2A and its mutants, H2AK118R and H2AK119R, were tested in *in vitro* ubiquitylation assays (Fig 4E). While disrupting the K118 residue had very little effect, K119R mutation resulted in a substantial loss of H2A ubiquitylation by the $CRL4^{WDTC1}$ E3 ligase. These results collectively suggest that $CRL4^{WDTC1}$ promotes H2AK119ub1 *in vitro* and *in vivo* in an adipocyte lineage-specific manner.

The most extensively characterized H2A E3 ligase is the RING1A/B of PRC1 complex which plays a critical and evolutionarily conserved role in developmental control in flies and mammals. It has been unclear whether and how a single E3 ligase regulates different biological processes that involve epigenetic silencing, especially when considering the abundance of H2AK119ub1 in cells (5–15% of total H2A). Two reports support the latter possibility, 2A-HUB (DZIP3/hRUL138) that mediates selective repression of a specific set of chemokine genes in macrophages [19] and $CRL4B^{RBBP4/7}$ that collaborates with PRC2 to repress various genes involved in cell growth and migration [20]. Our study supports the possibility that in addition to the historic PRC1, there may exist additional H2AK119 E3 ligases that function in epigenetic repression.

Multiple lines of genetic evidence from *Drosophila*, *C. elegans*, and mouse, and human epidemiology, have linked the function of WDTC1/Adp to the negative regulation of adipogenesis and fat metabolism. In this study, we demonstrate that the regulation of adipogenesis by WDTC1 requires its assembly into a CRL4 E3 ligase complex. A recent RNAi screen in *Drosophila* identified 47 genes which, when silenced, produced flies with high body fat (so-called antiobesity genes) [21]. Among them are *Cul4* and *Csn4*, which encodes a subunit of the COP9 signalosome that functions to activate CRL E3 ligases. These new findings provide additional support for the function of $CRL4^{WDCT1}$ as a negative regulator of adipogenesis and fat formation.

Materials and Methods

Plasmids

The human *WDTC1* (NM_015023.4) coding sequence was PCR-amplified from a HepG2 cDNA library and cloned into pENTR™/D-TOPO (Invitrogen) to generate a WDTC1 entry vector. $WDTC1^{\Delta H}$ was subcloned from pENTR-WDTC1 and $WDTC1^{RARA}$ was generated by sequential QuikChange site-directed mutagenesis (Stratagene) to pENTR-WDTC1. WDTC1 entry vectors were recombined with Gateway-adapted destination vectors (kind gift of Dr. K. I. Nakayama) p3XFLAG for transient and pMX-FLAG-puro for stable expressions. To generate WDTC1 knockdown-rescue vectors, shRNAs targeting mouse *Wdtc1* and shRNA refractory human *WDTC1* coding sequences were cloned into pLL-5.5-IRES-EGFP (kind gift of Dr. J. Bear), as described previously [18,22]. Mouse *Cul4a* and *Cul4b* shRNA sequences were designed using BLOCK-IT RNAi tool (Invitrogen) and cloned into pMKO.1-puro retroviral vector for stable knockdown of respective mRNAs in 3T3-L1 cells. All plasmids were sequence-verified, and shRNA oligos are listed in Table EV1.

Cell transfections, retroviral and lentiviral infections

293T cells were transfected at 1:3 plasmid-to-reagent ratio using Fugene 6 transfection reagent (Promega) for transient overexpression or transfected with 50 nM of siRNA for knockdown using Lipofectamine 2000 reagent (Invitrogen) according to manufacturers' protocols. Cells were incubated for 72 h for knockdown by siRNA; siRNA sequences were described previously [23] and listed in Table EV1. For retroviral or lentiviral production, 293T cells were

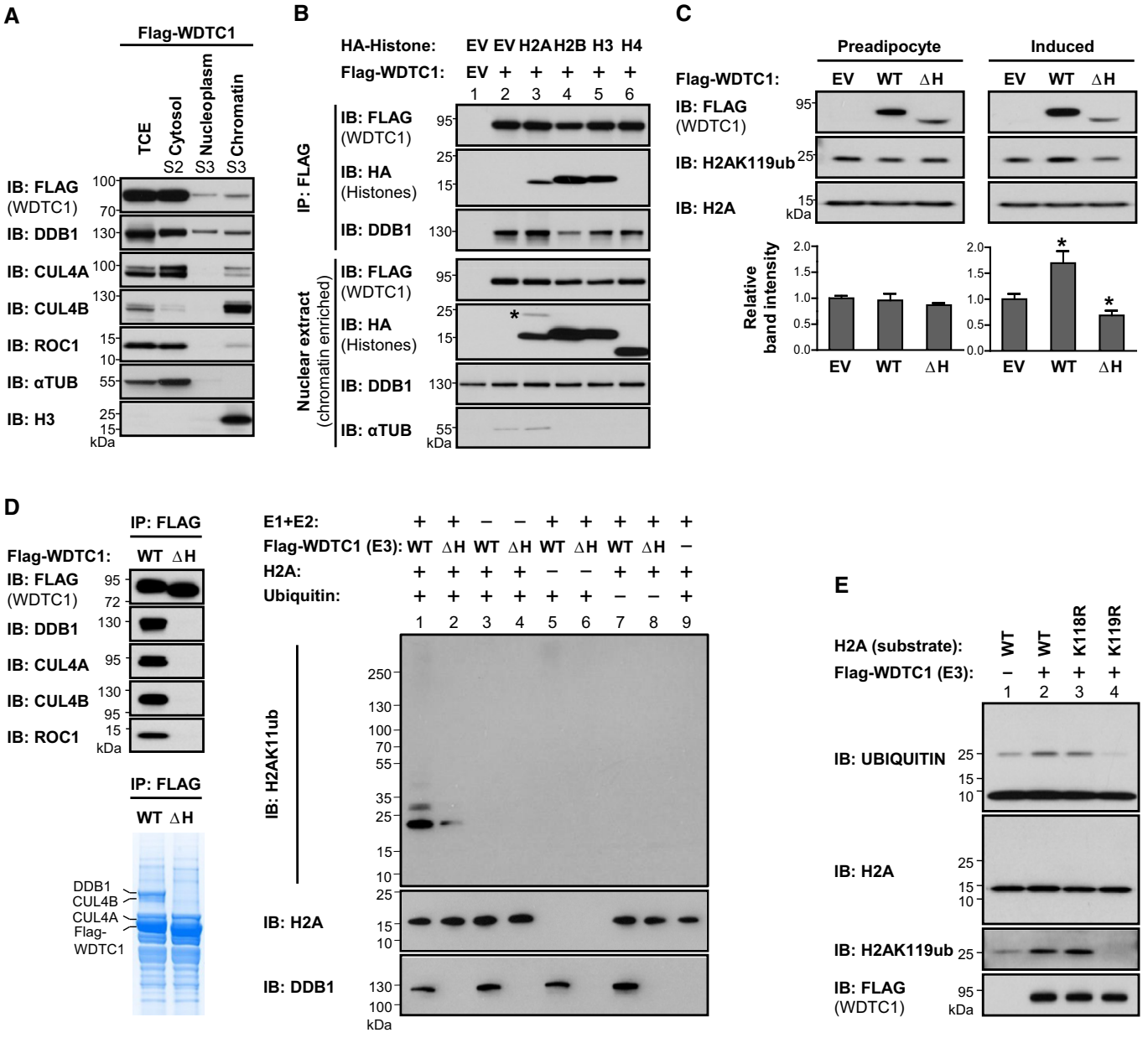

Figure 4. CRL4^{WDTC1} E3 ligase promotes H2AK119 ubiquitylation.

A Induced 3T3-L1 cells stably expressing Flag-WDTC1 were subjected to subcellular fractionation. Aliquots of total cell extract (TCE) and subcellular fractions were analyzed by immunoblot as indicated; fraction purity was assessed by α-tubulin and histone H3 antibodies.

B Chromatin-enriched nuclear extracts from 293T cells cotransfected with Flag-WDTC1 and HA-tagged core histones were immunoprecipitated (IP) with anti-FLAG and immunoblotted (IB) as indicated. The probable H2AK119ub1 band detected in the nuclear extract is indicated by an asterisk.

C Soluble chromatin extracts were prepared from preadipocyte or induced 3T3-L1 cells stably expressing control (EV) and Flag-WDTC1 proteins. H2A monoubiquitylation was detected by H2AK119ub1-specific antibody and total H2A served as a loading control. Relative intensity represents ratio of H2AK119ub1 over total H2A signal normalized to EV control.

D Affinity-purified Flag-WDTC1 wild-type and mutant ΔH complexes from 293T cells were the source of E3 ligase in *in vitro* ubiquitylation assays. Copurification of CRL4 E3 ligase proteins was confirmed by immunoblotting and Coomassie Blue staining (left panels). *In vitro* ubiquitylation assays of recombinant H2A were performed in the presence of the indicated proteins. Reaction products were resolved by SDS–PAGE, and ubiquitylated H2A was detected by anti-H2AK119ub1 (right panel).

E *In vitro* ubiquitylation assays were performed with purified wild-type and mutant histone proteins as substrates. H2A ubiquitylation was assessed by immunoblotting with anti-ubiquitin and various antibodies as indicated.

Data information: In (C), bars represent the mean ± SD from 2 (preadipocyte) or 3 (induced) independent experiments. *$P < 0.05$, significant change compared to EV control. Statistical significance (induced only) was analyzed by paired two-tailed Student's *t*-tests.
Source data are available online for this figure.

cotransfected with various plasmids for viral packaging as described [24]. For WDTC1 knockdown-rescue transfections, rescue vector plasmids were cotransfected with shRNA alone plasmids (2:1) for more complete knockdown of endogenous *Wdtc1* mRNA. Viral media was collected 48 h post-transfection at two 12-h intervals, syringe-filtered through 0.45-μm filter, and polybrene (8 μg/ml)-supplemented. Preconfluent 3T3-L1 preadipocytes were infected with the viral media twice within a 24-h interval. Cells were split to maintain preconfluency. Retrovirally transduced cells were selected with 4 μg/ml puromycin and maintained in selection media until adipogenic induction. Lentivirally transduced pLL-5.5-IRES-EGFP cells were visually selected for > 90% of cells with EGFP expression.

Antibodies, immunoprecipitation, and immunoblotting

A rabbit polyclonal antibody (Abgent, AP4944b) and a rabbit monoclonal antibody (Abcam, ab174294, [25]) were used to detect WDTC1. DDB1, CUL4A, and ROC1 antibodies were generated by our laboratory as described previously [23], and all other antibodies used in this study are commercially available and listed in Table EV2. Cells were lysed on ice with a NP-40 lysis buffer [50 mM Tris (pH 8.0), 150 mM NaCl, 10% glycerol, 1 mM EDTA, and 0.1% NP-40] supplemented with Halt™ (Thermo Sci.) protease/phosphatase inhibitor cocktail (PPIC). For immunoprecipitation experiments, clarified lysates prepared from Flag-WDTC1 expressing cells were immunoprecipitated by anti-FLAG M2 affinity gel (Sigma) overnight at 4°C. Immunoprecipitates were washed 3–5 times in lysis buffer with rotation, eluted by boiling in Laemmli buffer, resolved by SDS–PAGE, transferred to PVDF membrane (Millipore), and detected by immunoblotting with indicated antibodies. Immunoblotting was performed following standard protocols; blots were cut into strips to allow probing of the same gel with multiple antibodies when possible. Blots were developed using an ECL reagent (GE Amersham). Protein band densitometry analyses were performed using ImageJ software (U.S. National Institutes of Health).

3T3-L1 differentiation, Oil Red O staining, and triglyceride assay

3T3-L1 cells were cultured and differentiated as described previously [26]. 3T3-L1 preadipocytes were cultured in DMEM supplemented with 1× penicillin–streptomycin solution (Corning) and 10% (v/v) fetal calf serum (Colorado Serum Co.). To induce differentiation, 2 day post-confluent 3T3-L1 cells (day 0) were treated with an induction media containing 1 mM dexamethasone, 0.5 mM isobutylmethylxanthine (IBMX), and 1 μg/ml insulin (all from Sigma) in 10% fetal bovine serum supplemented DMEM. Two days later, induction media was replaced with 1 μg/ml insulin only for the duration of the experiment and media was changed every 2 days. A schematic summarizing 3T3-L1 differentiation with time points indicated for different experimental procedures is shown (Fig EV2B). To stain lipid droplets, cells were fixed in 3.7% buffered formaldehyde and stained with 0.3% Oil Red O. Triglyceride levels were measured with the Triglyceride Quantitation Kit and manufacturer's protocol (BioVision), and levels were normalized to sample protein concentrations by BCA assay (Thermo Sci.).

Real-time quantitative PCR

Total RNA was isolated from cells using Trizol (Invitrogen) and purified to remove residual phenol/chloroform using RNAeasy Mini cleanup (Qiagen). First-strand cDNA was synthesized with 800 ng of RNA using Superscript II reverse transcriptase kit (Invitrogen). Quantitative PCR (qPCR) was performed in duplicate using 1 μl of cDNA and SYBR Green PCR master mix (Applied Biosystems) in an Applied Biosystems 7900HT Fast Real-Time PCR system. Gene expression was normalized to *TPB* levels and analyzed by ΔΔCt method. qPCR primers for *Wdtc1* and *SREBP1c* were generated using Primer-BLAST (NCBI), and all other primers were reported previously [27,28] and listed in Table EV1.

Subcellular fractionation and chromatin extraction

Cell fractionation and soluble chromatin extraction by MNase digestion was performed as described previously [29]. Pelleted 3T3-L1 cells (8×10^6) were resuspended and incubated on ice for 5 min in 200 μl buffer A [10 mM HEPES (pH 7.9), 10 mM KCl, 1.5 mM $MgCl_2$, 0.34 M sucrose, 10% glycerol, 1 mM DTT and Halt™ PPIC] plus 0.1% Triton X-100. Nuclei were recovered in pellet 1 (P1) after centrifugation (4 min, 1,300 *g*, 4°C), and the supernatant (S1) was further clarified by centrifugation to obtain cytosolic fraction (S2). For nucleoplasmic fraction, P1 pellet was washed once in buffer A and lysed in 100 μl buffer B (3 mM EDTA, 0.2 mM EGTA, 1 mM DTT, and Halt™ PPIC), and centrifuged and the supernatant was recovered (S3). For chromatin-enriched fraction, P1 pellet was resuspended in buffer A and treated with 2 U MNase (1 min, 37°C) and centrifuged; treated nuclei were then lysed in 100 μl buffer B and the chromatin fraction was recovered in the supernatant (S3) of MNase treated nuclei. Immunoprecipitation with soluble chromatin extracts prepared by DNase treatment was performed as described previously [30].

In vivo and *in vitro* ubiquitylation assays

In vivo ubiquitination assays were performed as described previously [31]. For the detection of ubiquitylated WDTC1 *in vivo*, 293T cells were first transfected with HA-ubiquitin, split ~10 h later, transfected again with various combinations of plasmids and siRNAs at 24 h post-HA-ubiquitin transfection to minimize variations in HA-ubiquitin expression across plates. At 67 h post-siRNA transfection, cells were treated with MG132 (10 μM) and collected 5 h later. Cells were lysed under denaturing conditions in 1% SDS buffer [50 mM Tris (pH 7.5), 0.5 mM EDTA, 1% SDS, 1 mM DTT] by boiling for 10 min, and clarified lysate was immunoprecipitated in 0.1% SDS by 10-fold dilution with NP-40 buffer. Flag-tagged WDTC1 was immunoprecipitated by anti-FLAG M2 agarose beads, resolved by SDS–PAGE, and ubiquitylated WDTC1 was detected by immunoblotting with anti-HA antibodies. For *in vitro* ubiquitylation assays, WDTC1 immunocomplexes were purified from transiently transfected 293T cells expressing either Flag-WDTC1-WT or Flag-WDTC1-ΔH. Flag-tagged WDTC1 was immunoprecipitated with anti-FLAG M2 agarose beads overnight on a rotator at 4°C. Immunocomplexes were washed three times in lysis buffer and twice in TBS followed by elution with molar excess of Flag peptide

(Sigma). Ubiquitylation reactions were performed according to manufacturer's protocol using an ubiquitin conjugation kit (Enzo Life Sci.). In 50 μl reaction volume, unless noted otherwise in figure, 100 nM of either WT or ΔH immunocomplexes as the source of E3 and 200 nM of human recombinant histone H2A substrate (New England Biolabs) were combined with a ubiquitylation buffer containing 100 nM E1, 1 μM E2-UbcH5c, 1 μM human recombinant WT ubiquitin or ubiquitin Mutant No K (Boston Biochem), 1 U inorganic pyrophosphatase, 1 mM DTT, and 5 mM Mg-ATP. Reactions were incubated at 37°C for 30 min and terminated by addition of SDS sample buffer. Reaction products were resolved by SDS–PAGE and detected by immunoblotting with either anti-H2AK119ub1 or anti-ubiquitin antibodies.

Mass spectrometry

WDTC1-associated proteins were isolated from 3T3-L1 preadipocytes and induced adipocytes stably expressing Flag-WDTC1-WT and Flag-WDTC1-ΔH proteins by FLAG affinity purification, and cells transfected with an empty vector (EV) served as contamination controls for Flag immunoprecipitation. For analyses of interacting proteins in preadipocytes, WDTC1-WT and WDTC1-ΔH complexes were purified from ten 15-cm plates at day 0. For analyses of interacting proteins in induced adipocytes, day 0 preadipocytes were induced to differentiate and 2 days post-induction, WDTC1 complexes were purified from five (WT) or ten (ΔH) 15-cm plates; twice the number of cells were used in the purification of WDTC1-ΔH complexes due to its lower stable expression compared to WDTC1-WT. Cell pellets were lysed for 30 min on a rotating platform at 4°C in NP-40 lysis buffer [50 mM Tris (pH 8.0), 150 mM NaCl, 10% glycerol, 1 mM EDTA, and 0.1% NP-40] supplemented with Halt™ PPIC. Cell extracts were clarified by centrifugation, and the soluble fractions were incubated with anti-FLAG M2 agarose beads (Sigma) overnight on a rotating platform at 4°C. Immunoprecipitated proteins were washed ten times by inverting tubes in 10-ml wash volumes; five times in NP-40 buffer followed by five times in PBS. Protein complexes were eluted with 50 μl of 3XFLAG peptide (200 μg/ml) for 5 min by shaking (800 rpm) on a Thermomixer (Eppendorf) at 37°C; each sample was eluted three times and fractions were combined in a single tube on ice. A small amount of total purified protein (~2–5%) was resolved by SDS–PAGE and visualized by either silver staining or Coomassie Blue staining for confirmation. Eluted fractions were either in solution digested (preadipocytes) or in-gel digested (induced cells) at 37°C using trypsin (Promega). Digested peptides were desalted and purified by C_{18} resin (C_{18} columns or C_{18} Zip-Tip from Pierce or Millipore, respectively) following manufacturers' instructions. The identities of eluted proteins were determined by mass spectrometry analyses carried out at the UNC Proteomics Technology Development Core Facility using a LTQ-Velos-Orbitrap (Thermo Sci.) mass spectrometer coupled to a 2D nano-ultra-liquid chromatography system (Eksigent). The data were processed using MaxQuant software, and the MS/MS data sets were searched against UniProt mouse database. Processed data for Flag-WDTC1-WT and Flag-WDTC1-ΔH interacting proteins were manually sorted against contaminating proteins identified in EV control samples.

Sequence alignment

WDTC1 protein sequences from *Homo sapiens* (Hs), *Mus musculus* (Ms), *Xenopus laevis* (Xl), *Danio rerio* (Dr), *Drosophila melanogaster* (Dm), *Caenorhabditis elegans* (Ce), and *Arabidopsis thaliana* (At) were aligned to compare H-box sequence similarity in different species. Sequences were aligned using CLUSTAL 2.1 multiple sequence alignment tool.

Molecular modeling of WDTC1 and CRL4^{WDTC1}

Modeling was performed at the University of North Carolina R. L. Juliano Structural Bioinformatics Core. For modeling WDTC1, suitable templates for the H-box, WD40, and TPR domains of WDTC1 were identified using HHpred [32]. Three template structures were utilized as follows: WDTC1 H-box in complex with DDB1 (PDB 3I7N; [13]), DDB2 in complex with CRL4 (PDB 4A0K; [15]), and TPR domains of Sgt2 (PDB 3SZ7; [33]). The Hbox and WD40 domains were modeled simultaneously using the Modeller software package [34] and two template structures: PDB ID 3I7N and PDB: 4A0K. The TPR domains were modeled separately based on the template structure of Sgt2, a TPR structure from *Aspergillus fumigatus* (PDB ID 3SZ7). The model of the WDTC1-CRL4 complex was based on the structure of the DDB2-CRL4 complex (PDB ID 4A0K) with WDTC1 superimposed on and then replacing DDB2. The TPR domains were manually moved to a location near their insertion within the beta-propeller. Models were rendered using Pymol.

Expanded View for this article is available online.

Acknowledgements
We thank Dr. James Bear for providing pLL-5.5-IRES-EGFP plasmid and Dr. Brenda Temple for modeling WDTC1. We thank members of the Xiong laboratory, and Drs. William Marzluff and Brenda Temple for helpful discussions. This study was supported by U.S. National Institutes of Health grants NCI CPTAC 1U24CA160035 to X.C. and R01-GM067113 to Y.X.

Author contributions
BSG and YX designed research; BSG and FY performed experiments; MDS provided experimental support; YY and XC performed mass spectrometry analyses; and BSG and YX analyzed data and wrote the manuscript.

Conflict of interest
The authors declare that they have no conflict of interest.

References

1. Doane WW (1960) Developmental physiology of the mutant female sterile(2)adipose of *Drosophila* melanogaster. I. Adult morphology, longevity, egg production, and egg lethality. *J Exp Zool* 145: 1 – 21
2. Doane WW (1960) Developmental physiology of the mutant female sterile(2)adipose of *Drosophila* melanogaster. II. Effects of altered environment and residual genome on its expression. *J Exp Zool* 145: 23 – 41
3. Hader T, Muller S, Aguilera M, Eulenberg KG, Steuernagel A, Ciossek T, Kuhnlein RP, Lemaire L, Fritsch R, Dohrmann C *et al* (2003) Control of

triglyceride storage by a WD40/TPR-domain protein. *EMBO Rep* 4: 511 – 516

4. Suh JM, Zeve D, McKay R, Seo J, Salo Z, Li R, Wang M, Graff JM (2007) Adipose is a conserved dosage-sensitive antiobesity gene. *Cell Metab* 6: 195 – 207
5. Lai CQ, Parnell LD, Arnett DK, Garcia-Bailo B, Tsai MY, Kabagambe EK, Straka RJ, Province MA, An P, Borecki IB *et al* (2009) WDTC1, the ortholog of *Drosophila* adipose gene, associates with human obesity, modulated by MUFA intake. *Obesity (Silver Spring)* 17: 593 – 600
6. Galgani JE, Kelley DE, Albu JB, Krakoff J, Smith SR, Bray GA, Ravussin E (2013) Adipose tissue expression of adipose (WDTC1) gene is associated with lower fat mass and enhanced insulin sensitivity in humans. *Obesity (Silver Spring)* 21: 2244 – 2248
7. Pickart CM (2004) Back to the future with ubiquitin. *Cell* 116: 181 – 190
8. Hershko A (1983) Ubiquitin: roles in protein modification and breakdown. *Cell* 34: 11 – 12
9. He YJ, McCall CM, Hu J, Zeng Y, Xiong Y (2006) DDB1 functions as a linker to recruit receptor WD40 proteins to CUL4-ROC1 ubiquitin ligases. *Genes Dev* 20: 2949 – 2954
10. Angers S, Li T, Yi X, MacCoss MJ, Moon RT, Zheng N (2006) Molecular architecture and assembly of the DDB1-CUL4A ubiquitin ligase machinery. *Nature* 443: 590 – 593
11. Jin J, Arias EE, Chen J, Harper JW, Walter JC (2006) A family of diverse Cul4-Ddb1-interacting proteins includes Cdt2, which is required for S phase destruction of the replication factor Cdt1. *Mol Cell* 23: 709 – 721
12. Higa LA, Wu M, Ye T, Kobayashi R, Sun H, Zhang H (2006) CUL4-DDB1 ubiquitin ligase interacts with multiple WD40-repeat proteins and regulates histone methylation. *Nat Cell Biol* 8: 1277 – 1283
13. Li T, Robert EI, van Breugel PC, Strubin M, Zheng N (2010) A promiscuous alpha-helical motif anchors viral hijackers and substrate receptors to the CUL4-DDB1 ubiquitin ligase machinery. *Nat Struct Mol Biol* 17: 105 – 111
14. Rapic-Otrin V, Navazza V, Nardo T, Botta E, McLenigan M, Bisi DC, Levine AS, Stefanini M (2003) True XP group E patients have a defective UV-damaged DNA binding protein complex and mutations in DDB2 which reveal the functional domains of its p48 product. *Hum Mol Genet* 12: 1507 – 1522
15. Fischer ES, Scrima A, Bohm K, Matsumoto S, Lingaraju GM, Faty M, Yasuda T, Cavadini S, Wakasugi M, Hanaoka F *et al* (2011) The molecular basis of CRL4DDB2/CSA ubiquitin ligase architecture, targeting, and activation. *Cell* 147: 1024 – 1039
16. Nakagawa T, Xiong Y (2011) X-linked mental retardation gene CUL4B targets ubiquitylation of H3K4 methyltransferase component WDR5 and regulates neuronal gene expression. *Mol Cell* 43: 381 – 391
17. MacDougald OA, Lane MD (1995) Transcriptional regulation of gene expression during adipocyte differentiation. *Annu Rev Biochem* 64: 345 – 373
18. Uetrecht AC, Bear JE (2009) Golgi polarity does not correlate with speed or persistence of freely migrating fibroblasts. *Eur J Cell Biol* 88: 711 – 717
19. Zhou W, Zhu P, Wang J, Pascual G, Ohgi KA, Lozach J, Glass CK, Rosenfeld MG (2008) Histone H2A monoubiquitination represses transcription by inhibiting RNA polymerase II transcriptional elongation. *Mol Cell* 29: 69 – 80
20. Hu H, Yang Y, Ji Q, Zhao W, Jiang B, Liu R, Yuan J, Liu Q, Li X, Zou Y *et al* (2012) CRL4B catalyzes H2AK119 monoubiquitination and coordinates with PRC2 to promote tumorigenesis. *Cancer Cell* 22: 781 – 795
21. Baumbach J, Hummel P, Bickmeyer I, Kowalczyk KM, Frank M, Knorr K, Hildebrandt A, Riedel D, Jackle H, Kuhnlein RP (2014) A *Drosophila* in vivo screen identifies store-operated calcium entry as a key regulator of adiposity. *Cell Metab* 19: 331 – 343
22. Cai L, Marshall TW, Uetrecht AC, Schafer DA, Bear JE (2007) Coronin 1B coordinates Arp2/3 complex and cofilin activities at the leading edge. *Cell* 128: 915 – 929
23. Hu J, McCall CM, Ohta T, Xiong Y (2004) Targeted ubiquitination of CDT1 by the DDB1-CUL4A-ROC1 ligase in response to DNA damage. *Nat Cell Biol* 6: 1003 – 1009
24. Kotake Y, Cao R, Viatour P, Sage J, Zhang Y, Xiong Y (2007) pRB family proteins are required for H3K27 trimethylation and Polycomb repression complexes binding to and silencing p16INK4alpha tumor suppressor gene. *Genes Dev* 21: 49 – 54
25. Wu Y, Long Q, Zheng Z, Xia Q, Wen F, Zhu X, Yu X, Yang Z (2014) Adipose induces myoblast differentiation and mediates TNFalpha-regulated myogenesis. *Biochim Biophys Acta* 1839: 1183 – 1195
26. Student AK, Hsu RY, Lane MD (1980) Induction of fatty acid synthetase synthesis in differentiating 3T3-L1 preadipocytes. *J Biol Chem* 255: 4745 – 4750
27. Choi JH, Banks AS, Estall JL, Kajimura S, Bostrom P, Laznik D, Ruas JL, Chalmers MJ, Kamenecka TM, Bluher M *et al* (2010) Anti-diabetic drugs inhibit obesity-linked phosphorylation of PPARgamma by Cdk5. *Nature* 466: 451 – 456
28. van der Leij FR, Bloks VW, Grefhorst A, Hoekstra J, Gerding A, Kooi K, Gerbens F, te Meerman G, Kuipers F (2007) Gene expression profiling in livers of mice after acute inhibition of beta-oxidation. *Genomics* 90: 680 – 689
29. Mendez J, Stillman B (2000) Chromatin association of human origin recognition complex, cdc6, and minichromosome maintenance proteins during the cell cycle: assembly of prereplication complexes in late mitosis. *Mol Cell Biol* 20: 8602 – 8612
30. Day TA, Palle K, Barkley LR, Kakusho N, Zou Y, Tateishi S, Verreault A, Masai H, Vaziri C (2010) Phosphorylated Rad18 directs DNA polymerase eta to sites of stalled replication. *J Cell Biol* 191: 953 – 966
31. Hu J, Zacharek S, He YJ, Lee H, Shumway S, Duronio RJ, Xiong Y (2008) WD40 protein FBW5 promotes ubiquitination of tumor suppressor TSC2 by DDB1-CUL4-ROC1 ligase. *Genes Dev* 22: 866 – 871
32. Soding J (2005) Protein homology detection by HMM-HMM comparison. *Bioinformatics* 21: 951 – 960
33. Chartron JW, Gonzalez GM, Clemons WM Jr (2011) A structural model of the Sgt2 protein and its interactions with chaperones and the Get4/Get5 complex. *J Biol Chem* 286: 34325 – 34334
34. Fiser A, Sali A (2003) Modeller: generation and refinement of homology-based protein structure models. *Methods Enzymol* 374: 461 – 491